# Tidal forcing on David Glacier and Drygalski Ice Tongue

G. Casula,[1] S. Danesi,[1] M.Dubbini,[2] and L. Vittuari[3]

[1]Istituto Nazionale di Geofisica e Vulcanologia - Sez. Bologna, Via Donato Creti 12, 40128 Bologna ITALY (casula@bo.ingv.it, danesi@bo.ingv.it)
[2]DIMeC, Università di Modena e Reggio Emilia, Via Vignolese 905, 41100 Modena, ITALY (marco.dubbini@unimo.it)
[3]DISTART, Università di Bologna, Viale del Risorgimento 2, 40136 Bologna ITALY (luca.vittuari@mail.ing.unibo.it)

**Summary** During the 2005-06 Austral Summer, we carried out a joint observational campaign in the area of the David Glacier, South Victoria Land, with the aim of collecting simultaneous time series of geodetic and seismological data. We installed 7 temporary seismographic stations on rock outcrops surrounding the glacier and 3 temporary geodetic stations both on flowing ice and on rock. The seismic network registered a significant low-energy seismic activity, principally originated by ice creeping and basal stress at the interface between the ice and the bedrock. The geodetic stations allowed us to survey the glacier kinematics forced by the Ross Sea tides, and to infer the grounding line location. Here we show some details about data analysis and preliminary results.

**Citation:** Casula G., S. Danesi, M. Dubbini and L. Vittuari (2007), Tidal forcing on David Glacier and Drygalski Ice Tongue in the 10th ISAES X Online Proceedings, in Antarctica: A Keystone in a Changing World – Online Proceedings of the 10th ISAES X, edited by A. K. Cooper and C. R. Raymond et al., USGS Open-File Report 2007-1047, Extended Abstract 009, 4 p.

## Introduction

The David Glacier and its 90km-long floating extension (the Drygalski Ice Tongue) is the major drainage system of the Ross Sea eastern coast (Figure 1). Inland, the flow speed reaches 500-600 m/yr (Frezzotti et al., 1998) with large dependence on the topographical profile and the lubrication of the bedrock.

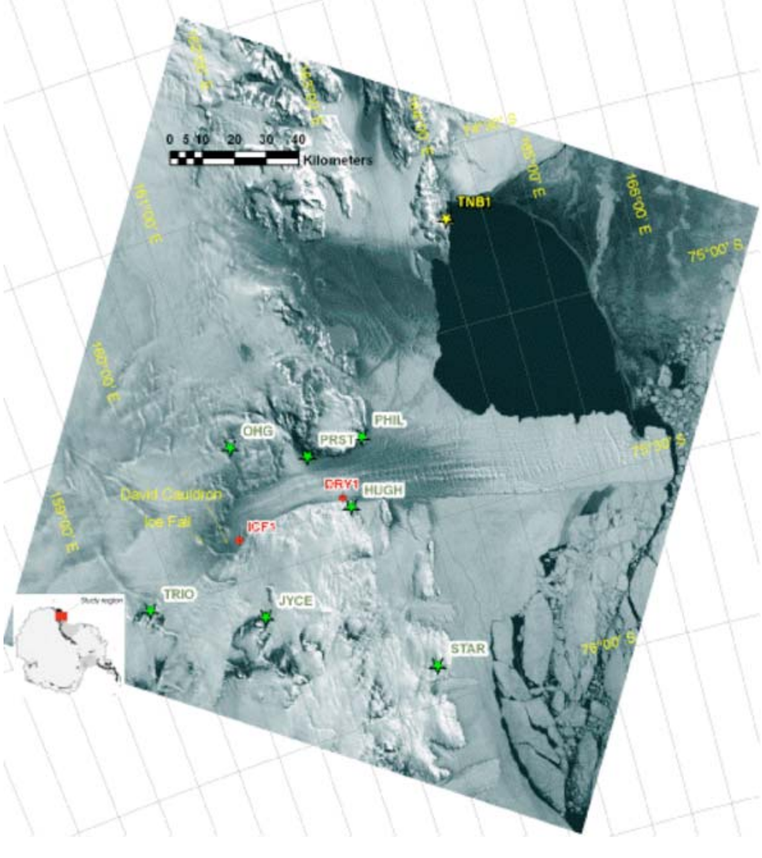

**Figure 1.** Satellite image of the region under study (ASTER-VNIR 2003) georeferenced to South Pole Polar Stereographic projection. The picture shows the deployment of the seismographic temporary stations (green stars) and GPS receivers (red circles). TNB1 (bigger yellow star) is the permanent geodetic Italian station operating close to the Italian scientific base MZS.

Low-magnitude local seismicity is commonly recorded and located beneath fast-flowing Antarctic ice streams and either ascribed to stress release across sticky patches or basal drag regime (Bahr & Rundle, 1996; Alley, 1992; Smith, 2006). The David Glacier seismic activity has been monitored and studied since 2003 (Danesi et al. 2007) in order to discriminate between possible tectonic and ice-related events.

On the kinetics point of view, any valid attempt to provide accurate time-space position of moving points on the glacier surface, necessarily invokes high-precision geodetical analyses (Frezzotti et al., 1998).

Therefore, the David-Drygalski system represent an excellent natural laboratory for joint geodetical and seismological data collection, in order to study possible correlations between vertical/horizontal glacier displacements and the weak typical seismic activity occurring inland beneath the ice stream.

## Data Collection and Analysis

During the Austral Summer 2005-06, we deployed a remote temporary network of 7 broadband seismographic stations and 3 GPS geodetic receivers, covering an area of about 100x150 km$^2$ around the David Glacier (Figure 1). The network operated continuously over three months (November 2005 to February 2006) recharged by solar panels (Figure 1).

Remote station locations are listed in Table1.

The seismic network was planned for two main reasons: the first goal was the continuous monitoring of the David Glacier local seismicity, but one additional reason was the investigation on possible correlations between the ice stream motion and earthquake occurrences.

Seismographic sites (green stars in Figure 1) were equipped with a 3-component broadband seismic sensor Trillium40 and a RefTek130 digital data logger. Two GPS geodetic stations, marked with red circles in Figure 1, were installed on the glacier at point ICF1 (inland) and DRY1 (on the floating ice tongue), equipped with Zephyr and Zephyr Geodetic antennas and dual frequency Trimble5700 GPS receivers. The primary master station for kinematics analysis was sited on a 3D benchmark on Hughes Bluff rocky outcrop, close to DRY1. As secondary Master station, we also used observations from the permanent GPS station (TNB1) sited next to MZS station, equipped with an Ashtech P code dual frequency receiver. In all cases, GPS data were collected on daily sessions at 15 sec rate and with 13° cut-off angle.

**Table 1 Geodetic and seismographic site locations**

| Site | Latitude (S) | Longitude (E) | Ellipsoidal Height (m) | Station Code |
|---|---|---|---|---|
| GPS Hughes | 75°23’52.68” | 162°12’06.18” | 165 | VLHG |
| GPS Drygalski | 75°21’45” | 162°08’15” | 37 | DRY1 |
| GPS Cauldron | 75°23’07” | 160°54’06” | 201 | ICF1 |
| GPS Permanent Station at MZS | 74°41’55.70” | 164°06’10.59” | 72.26 | TNB1 |
| Cape Philippi | 75°13’08.80” | 162°32’40.93” | 425 | PHIL |
| Hughes Bluff | 75°23’53.10” | 162°12’08.155” | 215 | HUGH |
| Mt Joyce | 75°37’05.55” | 160°53’27.80” | 1230 | JYCE |
| Mt Priestley | 75°13’25.38” | 161°54’32.37” | 475 | PRST |
| Ohg | 75°07’57.18” | 161°07’50.05” | 630 | OHG |
| Starr Nunatak | 75°53’56.36” | 162°35’33.235” | 70 | STAR |
| Trio Nunatak | 75°29’52.23” | 159°41’19.71” | 1145 | TRIO |

### *GPS data processing*

As pointed out by several authors (Anandakrishnan and Alley 1997, Anandakrishnan et al. 2002, Doake et al. 2002), GPS vertical and horizontal displacements on ice streams are often time correlated with solid earth and ocean tides. Moreover, the harmonic tidal analysis of GPS stations displacement measurements can be used to correctly determine the diurnal and semi-diurnal tidal components.

First, we inferred a reliable tidal model for this region from the analysis of data recorded during 1991, 1994 and 1995 scientific Italian campaigns in Antarctica, when tide gauges were operating close to MZS Italian base. It has been shown (Capra et al., 1999) that the estimate of 6 major tidal components (O1, K1, Q1, M2, S2 and N2) and 9 minor waves can nearly completely account for tidal amplitude values.

Then, we analyzed twelve days of GPS contemporaneous observations at ICF1 and DRY1 sites, recorded from January 15th to January 27th. The data sets used in this analysis were referred to the second Master station TNB1 (VLNDEF GPS Network) because of gaps in the VLHG data recordings. Position time series were computed with accuracy <10cm by using the TRACK1.15 module (Chen 1998, Herring 2002) of Gamit/Globk 10.3 package (King and Bock, 2000, Herring et al. 2006), which takes advantage from the sequential adjusting Kalman filter strategy. Starting from the ionospheric free linear combination and using IGS precise ephemeris, we found station coordinates, ambiguities and atmospheric biases for each GPS epoch.

Finally, we introduced GPS data into tidal harmonic analysis by using station displacement measurements as a tool to determine the diurnal and semi-diurnal tidal components. After data preprocessing, we used the GPS kinematics time series at temporary stations as input for the TSOFT software package (Van Camp and Vauterin, 2005) in order to remove outliers and offsets and interpolate gaps. A band pass filter was applied to decimate the data to 1 sample per minute and then to hourly sample rate.

The final step is the analysis of vertical displacements in order to obtain earth tide parameters (amplitude factors and phase lags) of the main tidal waves (O1, K1, Q1, M2, S2 and N2) in the least square sense.

### *Seismic data processing*

From the analysis of seismic data, we detected more then 4000 ice-related local events, mostly occurring within the ice layer and caused by ice deformation and ruptures. Only a few tens of events originated at the interface between the bedrock and the ice layer and were therefore named the *basal events*. The signal spectral analysis reveals a noteworthy dominance of low frequencies (<1Hz), amplified by the ice layer.

We initially located the hypocenters using the HYPOINVERSE algorithm (Klein, 2002), after that we relocated basal events with the Double-Difference approach (Waldhauser, 2001) that is particularly suited in the determination of high-precision relative locations (Danesi et al., 2007). Epicenters were sparsely spread around the topographic drop of a steep icefall where the slope is about 60%-80% (Rignot, 2002) and the flow is fast (more then 500m/yr from Frezzotti et al., 1998). Owing to uncertainties in the velocity model and to strong lateral heterogeneities, the seismic waveform propagation is still unmodeled and extremely challenging, so we cannot determinate the focal mechanism.

The magnitude for basal earthquakes was calculated, providing values in the range from 1.1 to 2.3 (see the procedure described in Danesi et al., 2007), with no evidence of the classical Gutenberg-Richter distribution of magnitude-frequency scaling.

## Discussion

Epicenter location and low-magnitude of basal events both point to basal drag stress concentration as main origin for these episodes, and exclude any tectonic origin (Danesi et al., 2007).

The magnitude of the observed episodes was too small to allow the detection of any possible surface seismic displacement. Our data suggest that the seismic contribution to the ice stream motion is negligible compared to the aseismic sliding. Nevertheless, GPS observations provided significant information about the glacier response to tidal forcing.

In Figure 2 the vertical movement of the site DRY1 and ICF1 derived from GPS kinematics data processing are represented together with the theoretical tidal displacement derived from the above-mentioned 15 waves model at MSZ.

The ratio of the sum of amplitudes of the two main diurnal tidal waves O1, K1 with respect to the semi-diurnal ones M2, S2 is about 2.72, meaning that the dominant pattern of the modeled tide is diurnal, and during a lunar day (24h 50m) only one high tide and one low tide can be observed.

The kinematics vertical displacement at site DRY1 exhibits periodic undulations of about 70cm following the trend of the synthetic tide, as expected.

On the contrary, the displacement at site ICF1 indicates a negative height variation, with reduced fluctuations, suggesting that the ice stream is grounded in this point, moving along the topographic slope towards the grounding line.

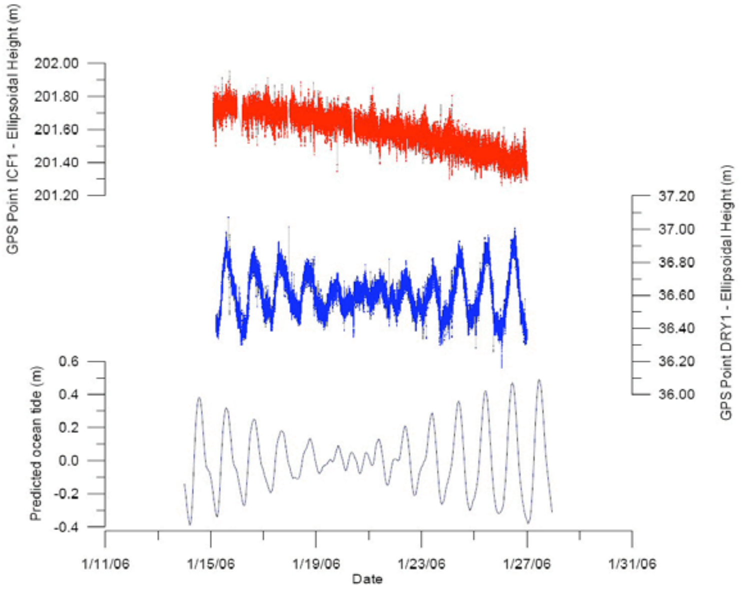

**Figure 2.** Comparison between the theoretical tidal displacement (solid black curve) and the vertical movement of the two GPS points, ICF1 (red curve) and DRY1 (blue curve).

## Summary

We present our preliminary results concerning the analysis of data recorded during a joint seismological and geodetical observational campaign, in the David Glacier area, Victoria Land, Antarctica. We principally focused our attention on the study of tidal forcing on the glacier and its floating ice tongue.

**Acknowledgments.** We are grateful to our colleagues for their assistance during field operations and network deployment, and to our co-editor Fred Davey. PNRA S.C.r.l., the Italian organization for research in Antarctica, provided field logistics and financial support. The satellite image in Figure1 ASTER-VNIR 2003/02/06 is a courtesy of U.S. Geological Survey (home page http:://www.usgs.gov).

## References

Anandakrishnan S. and R.B. Alley (1997), Tidal forcing of basal seismicity of ice stream C, West Antarctica, observed far inland, J. Geophys. Res., 102, B7, 15183-15196.

Anandakrishnan S., D.E. Voight, R.B. Alley, and M.A. King (2002), Ice stream D flow speed is strongly modulated by the tide beneath the Ross Ice Shelf, Geophys. Res. Lett., 30, 7, pp 1361-1364.

Alley, R.B. (1992), Sticky spots under ice streams, Antarc. J. of the U.S., 28, 5, pp 50-51.

Bahr, D.B. and J.B. Rundle (1996), Stick-slip statistical mechanics at the bed of a glacier, Geophys. Res. Lett., 23, 16, pp 2073-2076.

Capra A., S. Gandolfi, C. Lusetti, C. Stocchino, and L. Vittuari (1999), Kinematics GPS for the study of tidal undulations of floating ice tongue, Bollettino di Geodesia e Scienze Affini, IGM, LVIII, n. 2, pp 151-173.

Chen G. (1998), GPS Kinematics Positioning for the Airborne Laser Altimetry at long Valley, California, Ph. D. Thesis, Massachusetts Institute of Technology, pp. 173, Cambridge, MA.

Danesi, S., S. Bannister and A. Morelli (2007), Repeating earthquakes from rupture of an asperity under an Antarctic outlet glacier, Earth and Planet. Sc. Lett., 253, 1-2, 151-158.

Doake C.S.M., H.F.J. Corr, K.W. Nicholls, A. Gaffikin, A. Jenkins, W.I. Bertiger, and M.A. King (2002), Tide-induced lateral movement of Brunt Ice Shelf, Antarctica, Geophys. Res. Lett., 29 (8), pp 1226-1229, doi:10.1029/2001GL014606.

Frezzotti, M., A. Capra and L. Vittuari (1998), Comparison between glacier ice velocity inferred from GPS and sequential satellite images, Ann. Glaciol., 27, pp 54-60.
Herring, T.A. (2002), TRACK GPS kinematic positioning program, Version 1.07, Massachusetts Institute of Technology, Cambridge
Herring T.A., R.W. King and S.C. McClusky (2006), Gamit Reference Manual, GPS Analysis at MIT, Release 10.2.
King R.W. and Y. Bock (2000), Documentation for the GAMIT GPS Analysis Software, Dep. of Earth and Planetary Sciences, Massachusetts Institute of Technology, Cambridge, Scripps Institution of Oceanography University of California San Diego.
Klein F.W. (2002), User's guide to HYPOINVERSE-2000, a fortran program to solve for earthquake locations and magnitudes, U.S. Geol. Survey Open File Report, pp 2–171.
Rignot E. (2002), Mass balance of East Antarctic glaciers and ice shelves from satellite data, Ann. Glaciol., 34, pp 217-227.
Smith, A.M. (2006), Microearthquakes and subglacial conditions, Geophys. Res. Lett., 33, L24501, doi:10.1029/2006GL028207.
Van Camp M., and P. Vauterin (2005), Tsoft: graphical and interactive software for the analysis of time series and Earth tides, Computer & Geosciences, 31, pp 631-640.
Waldhauser F. (2001), hypoDD — a program to compute Double-Difference hypocentre locations, U.S. Geol. Survey Open File Report, 1–113.